EFDA–JET–PR(11)34

L. Frassinetti, M.N.A. Beurskens, R. Scannell, T.H. Osborne, J. Flanagan,
M. Kempenaars, M. Maslov, R. Pasqualotto, M. Walsh
and JET EFDA contributors

Spatial Resolution of the JET Thomson Scattering System

Spatial Resolution of the JET Thomson Scattering System

L. Frassinetti[1], M.N.A. Beurskens[2], R. Scannell[2], T.H. Osborne[3], J. Flanagan[2], M. Kempenaars[2], M. Maslov[4], R. Pasqualotto[5], M. Walsh[4] and JET EFDA contributors*

JET-EFDA, Culham Science Centre, OX14 3DB, Abingdon, UK

[1]School of Electrical Engineering, Royal Institute of Technology KTH, Association EURATOM-VR, SE-10044 Stockholm, Sweden
[2]EURATOM-CCFE Fusion Association, Culham Science Centre, OX14 3DB, Abingdon, OXON, UK
[3]General Atomics, P.O. Box 85608, San Diego, California 92186-5608, USA
[4]ITER Organization, CS 90 046, F-13067 Saint Paul lez Durance Cedex, France
[5]Consorzio RFX, Associazione EURATOM-Enea sulla fusione, Corso Stati Uniti 4, I-35127, Padova, Italy
** See annex of F. Romanelli et al, "Overview of JET Results", (23rd IAEA Fusion Energy Conference, Daejon, Republic of Korea (2010)).*

Preprint of Paper to be submitted for publication in
Review of Scientific Instruments

ABSTRACT

The instrument function of the High Resolution Thomson Scattering (HRTS) diagnostic in the Joint European Torus (JET) has been calculated for use in improved pedestal profile analysis . The Full Width at Half Maximum (FWHM) of the spatial instrument response is (22±1)mm for the original HRTS system configuration and depends on the particular magnetic topology of the JET plasmas. An improvement to the optical design of the laser input system is presented. The spatial smearing across magnetic flux surfaces is reduced in this design. The new input system has been implemented (from JET Pulse No's: 78742, July 2009) and the HRTS instrument function corresponding to the new configuration has improved to approximately FWHM = (9.8±0.8)mm. The reconstructed instrument kernels are used in combination with an ad-hoc forward deconvolution procedure for pedestal analysis as described in [6]. This procedure produces good results for both the old and new set-ups, but the reliability of the deconvolved profiles is greatly reduced when the pedestal width is of the same order as, or less than the FWHM of the instrument kernel.

I. INTRODUCTION

The High Resolution Thomson Scattering (HRTS) diagnostic on the Joint European Torus (JET) [4] started reliable routine operation in 2007. The HRTS diagnostic is a conventional 90° geometry system, which measures electron density (n_e) and electron temperature (T_e) profiles with up to 63 points along the outer radius of the plasma (R = 2.9-3.9m) at 20Hz. The diagnostic is particularly useful for measurement of the pedestal region in H-mode plasmas.

Depending on the scenario, the width of the pedestal in JET has been measured to be as small as ≈2cm for electron density and temperature [1, 2], a value very close to the spatial sampling of the HRTS system (≈16mm) in its original configuration. In the present configuration the spatial sampling is ≈8mm in the pedestal region, but the HRTS system's instrument function might still affect the measured pedestal width.

A careful study of the instrument function and of the related deconvolution techniques is essential in order to have a reliable estimation of the actual plasma pedestal width. The deconvolution is used to estimate the plasma pedestal width from the experimental measurement of the pedestal profile and is necessary when the pedestal width is comparable to the instrument function width. In this paper, the instrument function for the HRTS diagnostic in JET is numerically calculated and an application of a deconvolution method [6] is proposed.

The paper is organized as follows: Section II describes the geometry of the HRTS diagnostic. Section III describes the method of calculation of the instrument function, with a practical application on the original HRTS system configuration. Section IV discusses possible improvements of the system. Section V describes the instrument function for all the configurations used on JET, taking experimental uncertainties into account. The corresponding minimum pedestal width that can be measured by the HRTS diagnostic is discussed. In Section VI, the deconvolution techniques applied to the HRTS data and their limits are discussed. Conclusions are presented in Section VII. Finally,

Appendix A describes a simple analytical formula for the full width at half maximum (FWHM) of the instrument function.

2. GEOMETRY OF THE HRTS DIAGNOSTIC

A simplified schematic view of the HRTS system is shown in figure 1(a). The laser beam, which is focussed by a spherical and a cylindrical lens, enters the vacuum vessel through a window and terminates at a beam dump on the back wall. The beam is vertically elongated to reduce the power density below a threshold above which non linear stray light was detected. Light scattered from the plasma is collected by a linear array of optical fibres located vertically above the laser beam. For the calculation of the instrument function, the relevant geometrical parameters are: the laser beam trajectory through the plasma; the laser beam height at the window and at the back wall; the position of the viewing optical fibres, and the diameter (d) of the optical fibre collection cone of view along the laser beam path. For clarity, in figure 1 the collection cone is shown for a single fibre only. The coordinates (R,Z) that describe these parameters are illustrated in Figure 1(b) and summarized in Table 1. The diameter of the cone of view ($\delta = 12$mm) is determined by back-illuminating a fibre and measuring the diameter of the light spot onto the beam path. The laser beam height at the back wall is 119mm.

3. INSTRUMENT FUNCTION CALCULATION

In the system's original configuration (up to JET Pulse Number: 78742, in July 2009), a single scattering volume is formed from the light collected by two neighbouring fibres, as shown in Figure 2(a). The red and blue dashed lines represent the axis of the collection cone for two adjacent fibres. The continuous blue and red lines represent the borders of the collection cones. The horizontal lines correspond to the laser beam axis (dashed line) and the borders of the beam (continuous lines). The scattering volume is defined by the points P1, P2, P3 and P4. Along the laser path, each fibre's collection cone is 12mm in diameter with the axis of adjacent fibres separated by 8mm. Consequently, the collection cones for adjacent fibres overlap and the separation of the centre of mass for each experimental data point is approximately 16mm along the laser path.

Fibres looking at a different position along the laser path create a different geometry and hence different instrument functions. In the following, the instrument function for the scattering volume shown in Figure 2(a) is considered, which corresponds to the approximate position of the plasma pedestal ($R \approx 3.8$m).

The instrument function is calculated by considering several effects. At the most basic level, it can be seen that its width will lie between 20 – 36 mm at the pedestal, corresponding to the distances along the laser path from P3 to P4 and P3 to P2 at $R \approx 3.8$m, see figure 2(a).

The first step in evaluating the instrument function is to consider a laser beam with uniform intensity. The instrument function is numerically calculated with a series of line integrals across the scattering volume along a path perpendicular to the laser direction. The line integral is repeated

for all the radial positions from the abscissa of P3 to the abscissa of P2. The corresponding instrument function is shown in Figure 2(b), where the x coordinate follows the R coordinate and $x = 0$ corresponds to the abscissa of P3. For $x = 0$ to $x \approx 15$mm, the instrument function increases linearly from zero. Across the scattering volume enclosed by P1 to P4, the instrument function is approximately constant because the vertical height of the laser beam does not change significantly. As x further increases from the abscissa of P4 to P3, the instrument function linearly decreases to zero. The corresponding instrument function FWHM is 20.6mm

In order to obtain a more realistic estimation of the instrument function, the following items are incorporated into this basic model:

1) Since the magnetic field lines in the plasma are tilted with respect to the laser path, the line integral is performed along a line that has the same angle as the flux surfaces in the scattering volume. In principle, the angle changes with *x* and also depends on the plasma scenario. For simplicity, at this stage the angle α=85° is assumed, as the variation of α is negligible across the scattering volume.
2) A circular cross-section of the collection cone is considered. As a result, the simple line integral is replaced with a surface integral. The surfaces of integration correspond to the intersection of the flux surfaces with the scattering volume. Since the scattering volume is relatively small, the flux surfaces are approximated by planes parallel to the Last Closed Flux Surface (LCFS). The measured laser beam intensity profile is used. The incident laser is composed of two parallel beams and the spatial intensity profile of each beam is not uniform. On the right side of figure 2(a), the experimental beam intensity integrated in the toroidal direction is shown. The height of the beam in the Z direction is defined as the width of the experimental beam at its half maximum.
3) The corresponding instrument function is shown in Figure 2(c). The FWHM in this instance is 22.6mm. The most significant effect on the instrument function is due to the experimental beam intensity profile. Hereafter, all the instrument function calculations will be performed using tilted field line, circular fibres and the experimental beam intensity profile. Note that the FWHM depends on the plasma equilibrium as the field line angle varies with the plasma configuration.

4. IMPROVEMENT IN THE INSTRUMENT FUNCTION WIDTH

As stated above, the instrument function FWHM for the original configuration of the HRTS diagnostic is calculated to be ≈2.2cm in the pedestal region ($R \approx 3.8$m). Consequently, in order to resolve pedestal widths smaller than ≈2cm it is necessary to look at possible ways of reducing the FWHM of the instrument function. In this section the improvements that can be obtained by modifying the scattering volume are discussed.

The scattering volume depends on the diameter δ of the cone of view of the optical fibres on the laser path and on the height of the laser beam. The diameter δ cannot be easily modified, but the

scattering volume can be reduced by using the light collected by a single fibre only. Using a single fibre also reduces the spatial sampling from ≈16mm to ≈ 8mm. The height of the laser beam can be modified by changing the input lenses. Therefore, the change to a single fibre and the careful selection of a lens with a new focal length are the tools available to reduce the instrument function width.

4.1. A) USING A SINGLE FIBRE

In its original configuration, the HRTS scattering volume is formed from light collected by two adjacent fibres. As such, it may seem clear that using the light collected by a single fibre will strongly reduce the FWHM of the instrument function. However, this is not always the case in the pedestal region, as shown in Figure 3(a) where the FWHM is plotted *vs*. the radial position of the scattering volume. The first thing to note is that the FWHM is dependent on the radial position, and increases towards the pedestal region. This is related to the variation along the radius of the angle of the fibre collection cone relative to the laser path. In the core region, the collection cone is almost vertical and the scattering volume is smaller than at the pedestal, where it is significantly tilted. The FWHM is ≈1.6cm at R≈3.0m and ≈2.3cm at R≈3.9m, see the red continuous line in Figure 3(a). Note that the FWHM is approximately constant from R≈2.9m up to R≈3.3m but then it increases almost linearly. This transition is due to a geometrical effect. Appendix A shows that the radial position at which the transition occurs (r_c) is related to the diameter of the collection cone δ and to the height h of the laser beam via $r_c=R_0+H\delta/h$ (where R_0 is the abscissa of the fibres and at H the distance of the fibres from the laser path). Before r_c, the FWHM is constant and depends on the collection cone diameter, $FWHM \approx \delta$. After r_c, the FWHM increases linearly with R and depends on the height of the laser beam, $FWHM \approx (R-R_0)h/H$.

The FWHM of the instrument function calculated by considering the scattering volume formed by a single collection cone is shown by the blue dashed line in Figure 3(a), In the core region, the reduction of the FWHM is significant; from ≈1.6cm (double fibre) to ≈1.0cm (single fibre). In fact, in the core the cone of view is almost vertical and the instrument function depends mainly on the width of the scattering volume along the laser path. In the pedestal region the reduction is minimal, from ≈2.3cm to ≈2.1cm. In this region the cone of view is significantly tilted and the instrument function depends mainly on the laser beam height. Note that in the single fibre case the transition radius r_c is located in a radial position inner than in the double fibre case and that the FWHM increases continuously with radius.

4.2. B) CHANGING THE FOCAL LENGTH OF THE INPUT LENS.

Anther way to reduce the scattering volume is to decrease the height of the laser beam. The height of the laser beam is determined by the focal length of the lens pair located at R = 8.36m, as shown in Figure 1(a). In the original configuration, a spherical lens with focal length f = 4.5m and a cylindrical lens with f = 4m combine to produce a 119mm beam height on the back wall.

A change of the cylindrical lens does not affect the required collection cone as the depth of focus is long enough in the vertical direction. Figure 3(b) shows the expected instrument function FWHM at the pedestal calculated as function of focal length of the cylindrical lens. The effect of focal length is analysed from f = 3.5m to f = 11m. The reduction of the FWHM with the increase of the focal length is evident. Note that no significant improvement is obtained beyond f ≈ 10m. Appendix A qualitatively shows that the reduction of FWHM is geometrically limited by the diameter of the collection cone of view. From figure 3(b), the minimum FWHM that can be obtained by changing the lenses is approximately 16mm for the double fibre case and 10mm for the single fibre case.

In Figure 3(c), the FWHM of the instrument function as function of the major radius is calculated by assuming f = 10m for the cylindrical lens. This focal corresponds to a 60mm laser height at the back wall, sufficiently large to avoid exceeding the stray light threshold. The difference with the case f = 4 in figure 3(a) is significant: the FWHM is smaller and is constant across the major radius for both double and single fibre. This shows that reducing the beam height can greatly minimise the radial dependence of the instrument function width. Moreover, the change from a double fibre to a single fibre scattering volume results in a significant reduction in the width of the instrument function, across the entire HRTS profile, including the pedestal region. For this example, the FWHM of the instrument function is reduced from ~1.6cm to ~1.0cm. The dots in figure 3(b) highlight the three different configurations that have been used at JET. For completeness, figure 3(d) shows the dependence of the FWHM on the angle of the magnetic field line at the pedestal. In the original HRTS configuration (double fibre and f = 4m), the magnetic field line angle has a significant impact on the FWHM. In the new configuration (single fibre and f = 10m), the field line angle θ has a significant effect only for θ <80°.

5. PRESENT CONFIGURATION

In order to minimise the FWHM, as of July 2009 (JET Pulse No: 78742), the HRTS configuration has been changed by using a cylindrical lens with focal length f = 10m and using a scattering volume formed by a single fibre in the pedestal region (for R>3.73m). Note that the use of a single fibre not only reduces the instrument function FWHM, but also increases the spatial sampling of the HRTS data: in the pedestal region, the HRTS data points are separated by 8mm while in the core (R<3.73m) data points are separated by 16mm.

In figure 4(a) the instrument function calculated at R = 3.8m for the original configuration is shown. In figure 4(b) the instrument function calculated at R = 3.8m for the present configuration (single fibre and f = 10m) is shown. Field line angle θ = 85°is assumed.

To more accurately determine the instrument function for the configurations used in JET, a Monte Carlo procedure has been used in order to estimate the effects of the uncertainties on the height of the laser beam (uncertainty 2mm), on the diameter of the collection cone of view along the laser path (1mm) and on the angle of the LCFS (2°). In simple terms, the instrument function is calculated 100 times with random changes applied to the beam height, the cone diameter and the

LCFS angle within their experimental errors. The grey areas in figure 4 show the range of variation (from the 5th to the 95th percentile) of the instrument function and the red lines show the average value. The corresponding FWHM are *(22±1) mm* for the original configuration and *(9.8±0.8)mm* for the present configuration. The case of double fibre and f = 10m (corresponding to the present configuration for R<3.73) has *FWHM = (15±1)mm*

An important issue to consider is the minimum pedestal width that can be measured for a given instrument function. This is evaluated by convolving a 'real' pedestal profile with zero width (i.e. a step-like profile) with the instrument function. The minimum measurable pedestal width is then calculated by fitting the convolved profile with a modified hyperbolic tangent function (*mtanh*) [Groebner-2002]. The results are plotted as dashed lines in Figure 5. The minimum pedestal width is very close to the corresponding FWHM instrument function (dot-dashed line in figure 5). This kind of calculation assumes an infinite number of experimental data points across the profile, which matches well to the situation where a radial shift is applied [Beurskens-2009]. With a radial shift, the plasma is slowly moved in the radial direction by some cm during the H-mode phase. Therefore, it is possible consider simultaneously several profiles, each one radially translated for the corresponding shift in order to obtain a profile with a very small spatial sampling.

But when only a single profile is considered, a limited number of experimental points are available in the pedestal region. To obtain an accurate estimation of the minimum pedestal width, the convolved profile is sampled at the positions of the experimental measurements. Then, the fitting is performed using the sampled profile. In the double fibre case, only 2-3 measurements are available in the region where the convolved pedestal is located. For the single fibre case, approximately 4-5 measurements are available. Results are shown by the continuous lines in Figure 5. Oscillations in the minimum pedestal width are due to the fact that the number of data points in the pedestal region depends on the pedestal position. In the case of the single fibre configuration, the oscillation is very small since the double of data is available. In general, when a single profile is considered, the minimum measurable pedestal width is larger than the case with several radially-shifted profiles.

6. DECONVOLUTION OF ELECTRON DENSITY AND ELECTRON TEMPERATURE PROFILES.

The relatively new deconvolution technique presented in reference [6] requires only the knowledge of the instrument function and of the measured T_e and n_e profiles.

The width of instrument function can strongly affect the measured width of the pedestal. This effect is almost negligible if the pedestal width is much larger than the instrument function's FWHM, but can be significant when the pedestal width is similar or lower than the FWHM of the instrument function. In this section we describe the technique (and its limitation) that is used to deconvolve the measured profiles in JET, i.e. to estimate the actual plasma profiles (n_e^{plasma} and T_e^{plasma}) from the measured profiles ($\hat{n}_e$ and $\hat{T}_e$) once instrument function effects are taken into consideration. The goal is to obtain the *mtanh* fitting parameters of the actual plasma profiles starting from the

measured profiles and the instrument function. Hereafter, the *mtanh* fitting parameters are defined by the vectors a_{ne} and a_{Te} for density and temperature respectively.

The measured density $\hat{n}_e$ can be approximated as the convolution of the plasma density with the instrument function *I(r)* over the scattering length ΔR:

$$\hat{n}_e = \int_{\Delta R} n_e^{plasma}(r) \cdot I(r) dr \qquad \text{(VI.1)}$$

To calculate a_{ne}, the measured density $\hat{n}_e$ is fitted with a function defined as the *mtanh* convolution with the instrument function:

$$n_e^{fit}(r, a_{ne}) = \int_{\Delta R} mtanh(r, a_{ne}) \cdot I(r) dr \qquad \text{(VI.2)}$$

For the temperature the situation is more complicated because the measured temperature is weighted to the density profile [Scannell-2006, Scannell-2011]. An effect of the weighting is that the measured temperature profile has a pedestal position more external than the actual pedestal position. A reasonable approximation for the measured temperature is then:

$$\hat{T}_e = \frac{\int_{\Delta R} T_e^{plasma}(r) \cdot n_e^{plasma}(r) \cdot I(r) dr}{\int_{\Delta R} n_e^{plasma}(r) \cdot I(r) dr} \qquad \text{(VI.3)}$$

Note that an alternative density weighted temperature, in which the square root of T_e^{plasma} is used in equation VI.3, can be obtained assuming that the dominant factor in the measured temperature is the spectrum width. Since it is proved that the two different weighing methods do not produce significant differences [6], equation VI.3 is used for simplicity. Therefore, the fitting parameters of the plasma temperature profile a_{Te} are calculated by fitting the measured temperature with the function:

$$T_e^{fit}(r, a_{Te}, a_{ne}) = \frac{\int_{\Delta R} mtanh(r, a_{Te}) \cdot mtanh(r, a_{ne}) \cdot I(r) dr}{\int_{\Delta R} mtanh(r, a_{ne}) \cdot I(r) dr} \quad , \qquad \text{(VI.4)}$$

where the parameters a_{ne} have been calculated using the fitting function VI.2.

For the density, the main difference between the measured and the plasma profile is in the pedestal width, due to the convolution with the instrument function. For the temperature, the main differences are in the pedestal width, due to the deconvolution, and in the pedestal position, due to the density weighting.

To verify how close the estimated fitting parameters are to the real plasma parameters, a simulation is performed. The input profiles to this simulation are *mtanh* pedestal profiles for density and temperature of varying widths. From these original profiles, the measured profiles are obtained by the four-channel polychromators signals calculated using the actual HRTS system's filter layout

and the theoretical Thomson scattering spectrum. The parameters a_{ne} and a_{Te} are estimated using equations VI.2 and VI.4 and compared to the original parameters.

This procedure is done using the instrument function calculated for the original HRTS configuration: results are shown in figure 6. The shaded areas represent the uncertainty corresponding to a 10% error in the instrument function FWHM. In the left column, the ratio between the estimated pedestal width and the original pedestal width is shown versus the original pedestal (green dots). For comparison, the convolved width, i.e. the width corresponding to the measured profiles, is shown with purple dots. The original width is well estimated as long as it is larger than the FWHM (22mm). For the widths smaller than the FWHM, the uncertainty introduced
by the deconvolution (the shaded area) is significant. On the right column, the difference between the estimated pedestal position and the original pedestal position is shown. For the measured density no difference in the pedestal position is observed. For the measured temperature, even if a difference in the measured pedestal position is introduced, the deconvolution allows a reasonable estimation of the original position for all the widths.

A similar study is performed using the present HRTS settings in figure 7. In this case, the original pedestal width can be reliably estimated down to 1cm.

As a practical application of this technique, in figure 8 we show the experimental temperature and density profiles (red dots) along with the non-deconvolved *mtanh* fits (black dashed lines) and the deconvolved fits (continuous blue line). The profiles are radially shifted in order to take into consideration the spatial displacement introduced by the radial movement of the plasma [1, 2].

Figure 8(a) and 8(b) correspond to the profiles for a shot measured with the original HRTS configuration, i.e. with an instrument function characterized by FWHM ≈ 22mm. The effect of the deconvolution is evident on the pedestal width, both for the temperature and the density profiles. The deconvolved width is approximately 2cm and 1cm smaller than the non-deconvolved width for temperature and density respectively. For the temperature profile, it is also evident the difference in the pedestal position, as above discussed.
Figure 8(c) and 8(d) correspond to the profiles for a shot measured with the present HRTS configuration, i.e. with an instrument function characterized by FWHM ≈ 11mm. With this configuration and for these profiles, the effect of the instrument function is smaller. The deconvolved temperature pedestal width is 5mm smaller than the non-deconvolved one. For the density pedestal width the difference is even smaller, around 3mm.

CONCLUSIONS

Within this paper, the instrument function of the HRTS diagnostic in JET has been investigated for the main relevant configuration. For the system's original configuration the FWHM of the instrument function is found to be (22±1)mm within the pedestal region. By investigating the key parameters effecting the width of the instrument function and making strategic changes to the system configuration, this value has been reduced to (9.8±0.2)mm, with the exact value depending

on specific plasma magnetic configuration. It has been shown that an instrument function with a FWHM similar to the diameter of the fibre collection cone is the best result that can be obtained.

The capabilities of the deconvolution techniques used in JET are discussed. For pedestal widths smaller than the FWHM, the uncertainty on the deconvolved width is significant. The deconvolution is able to obtain a reliable estimation of the real pedestal width as long as its value is not smaller than the FWHM of the instrument function.

A practical example shows that with the original HRTS configuration the instrument function can have a drastic impact on the estimated pedestal width. With the present HRTS configuration the instrument function effect minimal.

APPENDIX A:
A QUALITATIVE ANALYTICAL FORMULA OF THE INSTRUMENT FUNCTION FWHM

The instrument function FWHM can be analytically determined using some assumptions.

1) The fibers are located at a distance H>>a from the laser path, where a is the plasma minor radius
2) the collection cone of view can be approximated with a cylinder
3) The fiber cross section is rectangular and not circular
4) The beam height h is constant along the entire beam path
5) The beam intensity is uniform
6) The flux surfaces are perpendicular to the laser beam.

Given these simple assumptions, the instrument function FWHM is determined by three parameters only: the height of the laser beam h, the diameter of the cone of view δ on the laser path and the angle a between the laser path and the cone of view.

Consider the scattering volume defined by the points P1, P2, P3 and P4 determined by the intersection of the laser beam with the collection cone of view. Two relevant geometries are possible. First, the collection cone of view can be almost vertical and the P1 abscissa is located between P3 and P4, see the Figure 9(a). This case corresponds to the geometry in the core region. In Figure 9(a), L is the distance on the horizontal axis between P3 and P2 and l between P1 and P4. The instrument function is calculated by performing the line integral along vertical lines and the result is sketched in Figure 9(b). The instrument function is a trapezium with $FWHM = (l+L)/2$. Then, by looking at the geometry of Figure 8(a) it is possible to calculate: $l = \delta - h/tg\alpha$ and $l = \delta + h/tg\alpha$ so that:

$$FWHM = (l + L) / 2 = \delta \qquad \text{(A.1.)}$$

Therefore the FWHM corresponds to the diameter of the cone of view and is independent from the beam height and from any other quantity.

Second geometry, the cone of view can be strongly tilted, so that the abscissa of P1 does not fall between P3 and P4. See Figure 9(c). This case can be relevant in the pedestal region. The expression

for l and L are: $l = -\delta + h/tg\alpha$ and $l = \delta + h/tg\alpha$ so that $FWHM = (l + L) / 2 = h/tg\alpha$.

The FWHM depends on the height of the laser beam and on the scattering angle. If the fibres are located at the abscissa R_0 and at distance H from the laser path, then the radial position of the scattering volume is $R \approx R_0 + H/tg\alpha$. Therefore, the FWHM in case 2 increase linearly with the radius R:

$$FWHM = (R - R_0)h/H. \qquad \text{(A.2)}$$

The angle of transition α_c from case 1 to case 2 is $\alpha_c = atan(h/\delta)$ which corresponds to the radial position $r_c = R_0 + H\alpha/h$.

The trend of the FWHM is sketched in Figure 9(e). If the fibre diameter is reduced (for example by passing from the double fibre settings to a single fibre), the transition occurs earlier. If the beam height is reduced (for example by changing the lens) the transition can be moved outside the plasma and the FWHM becomes approximately independent of the radial position of the scattering volume. Note the qualitative similarity with Figure 3(a). According to this model, the FWHM is limited by the collection cone of view diameter.

ACKNOWLEDGEMENT.

This work was supported by the European Communities under the contract of Association between EURATOM and VR and was carried out within the framework of the European Fusion Development Agreement. The views and opinions expressed herein do not necessarily reflect those of the European Commission.

REFERENCES

[1]. M.N.A. Beurskens et al, 2009 Plasma Physics and Controlled Fusion **51**, 124051
[2]. M.N.A. Beurskens et al, 2011 Physics of Plasmas **18**, 056120
[3]. R.J. Groebner et al, 2002 Plasma Physics and Controlled Fusion **44** A265–A272
[4]. R. Pasqualotto et al, 2004 Review of Scientific Instruments **75**, 3891
[5]. R. Scannell et al, 2006 Review of Scientific Instruments **77**, 10E510
[6]. R. Scannell et al, 2011 Review of Scientific Instruments **82**, 053501

	R (mm)	**Z (mm)**
a	7935	327
b	1727	−59.5
c	7935	283
d	1727	59.5
e	2920	3772.5

Table 1: *Geometry corresponding to the HRTS system original configuration. Letters correspond to the points in Figure 1(b).*

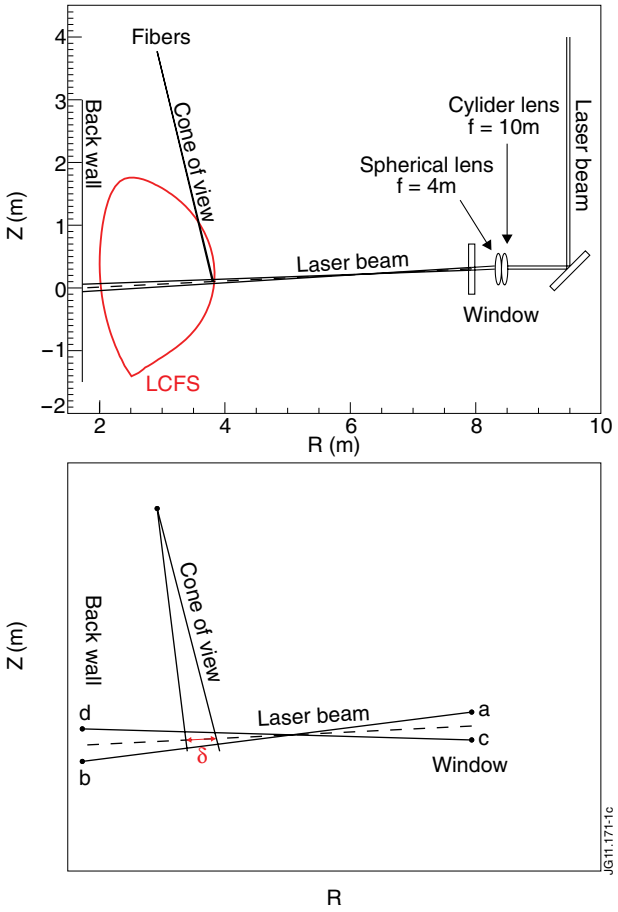

Figure 1: (a) Geometry of the HRTS diagnostic. (b) Schematic view of the geometry used in the instrument function calculation.

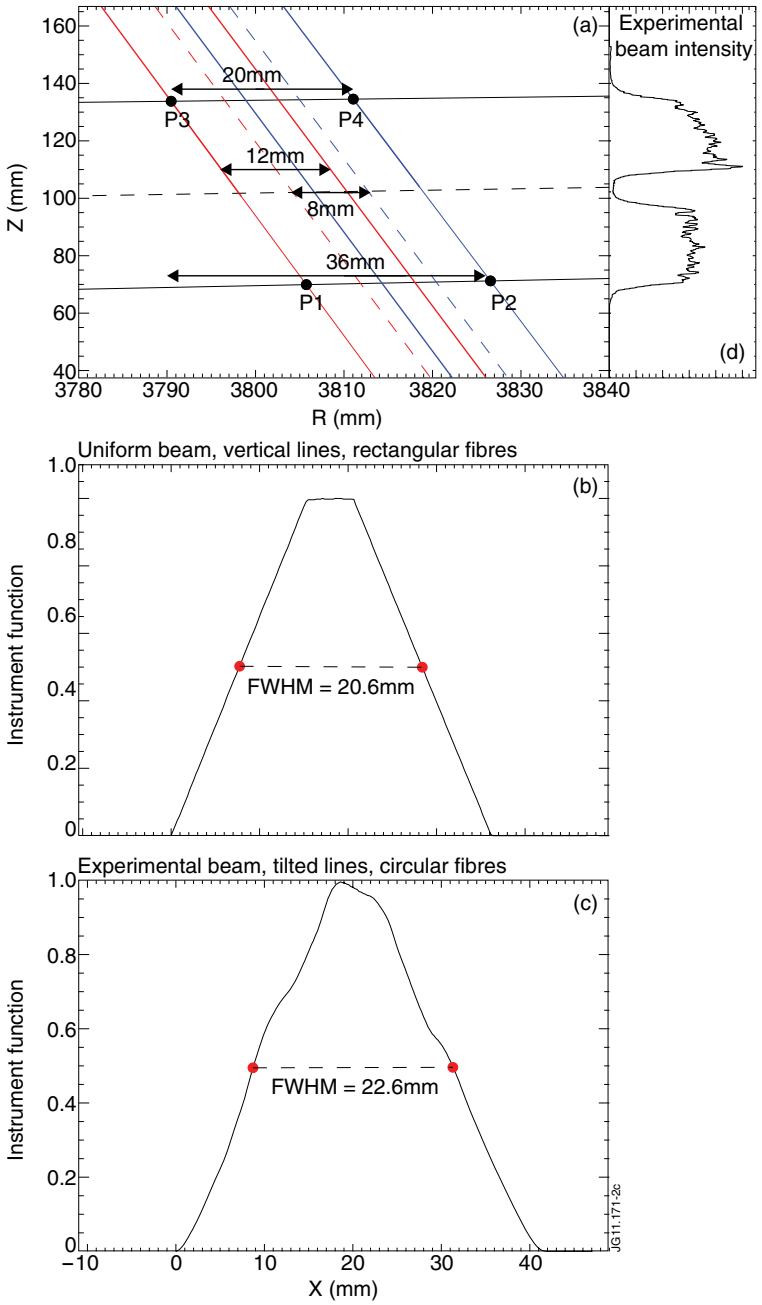

Figure 2: (a) Geometry of the scattering volume in the pedestal region. Black lines show the laser beam path. Coloured lines the path of two adjacent cones of view. The dashed lines correspond to the axis of the beam and of the cones of view. (b) Instrument function calculated assuming vertical field lines, rectangular section of the cones of view and uniform intensity of the laser beam. (c) Instrument function calculated assuming tilted field lines, circular section of the cones of view and experimental intensity of the laser beam.

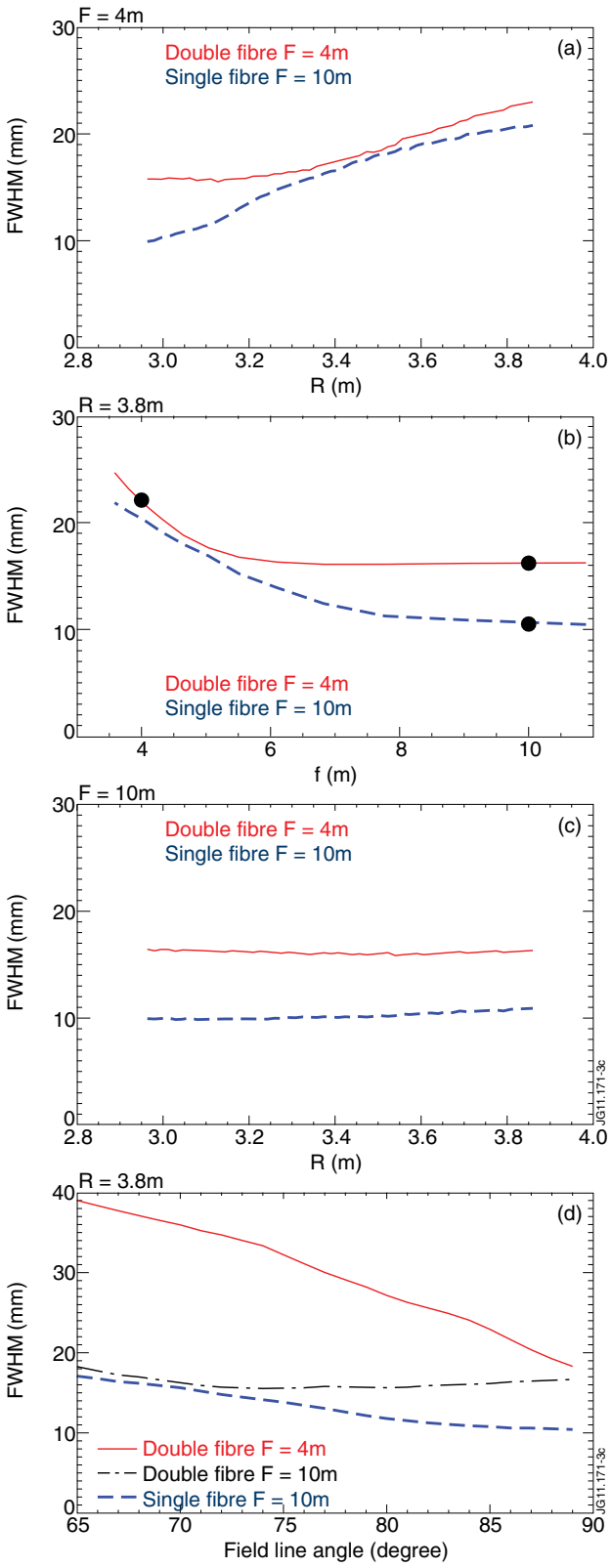

Figure 3: (a) Instrument function FWHM versus the radial position of the scattering volume for a laser beam with focal length f = 4m. (b) FWHM versus the focal length at the pedestal. Dots highlight the three different configurations at JET. (c) FWHM versus radius using focal length f = 10m. (d) FWHM at R = 3.8m versus the field line angle.

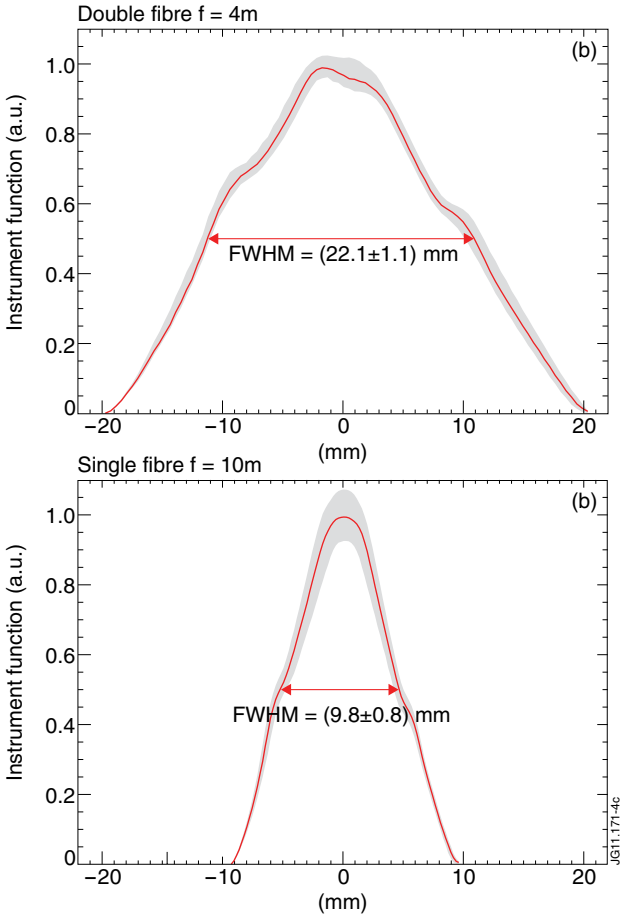

Figure 4: Instrument function at R = 3.8m calculated for the original configuration (a) and the present configuration (b). The shaded areas highlight the range of variation of the instrument function due to the uncertainties on the laser beam height, cone of view diameter and angle of the field lines.

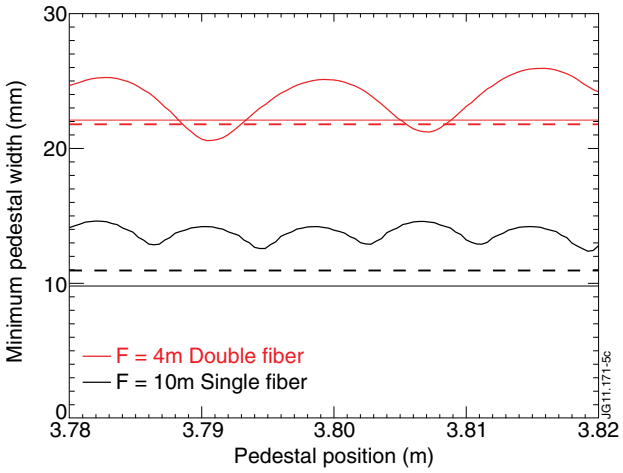

Figure 5: Minimum measureable pedestal width versus pedestal position. Continuous lines correspond to a single profile case, dashed lines to multiple radially-shifted profiles and dot-dashed line to the FWHM.

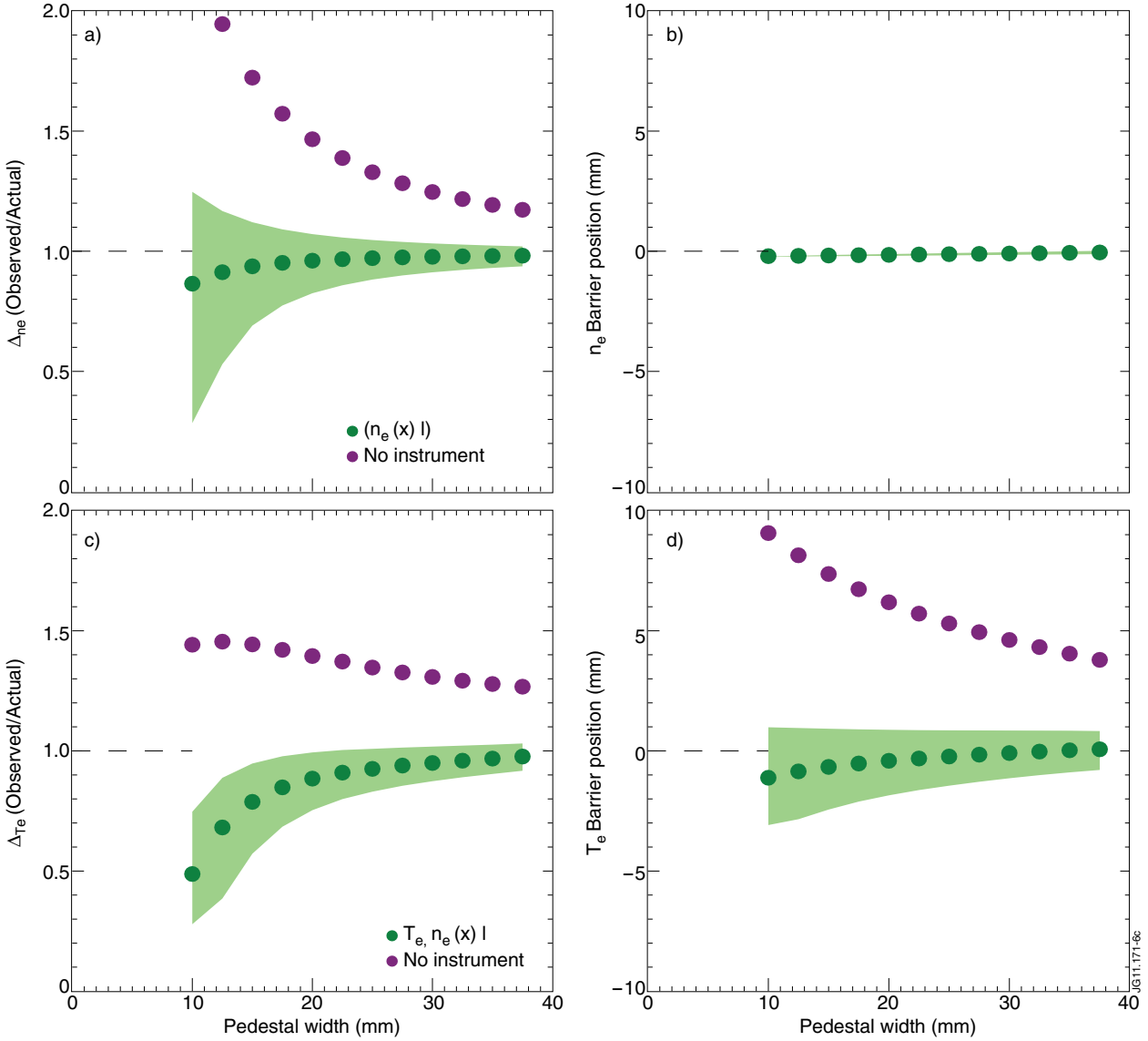

Figure 6: Simulation results using the original HRTS configuration (double fibre, f = 4m) for the pedestal fits without (purple) and with deconvolution (green dots) for (a) density pedestal width, (b) density pedestal position, (c) temperature pedestal width, (d) temperature pedestal position. Shaded areas represent the uncertainty estimated using a 10% error on the instrument function FWHM.

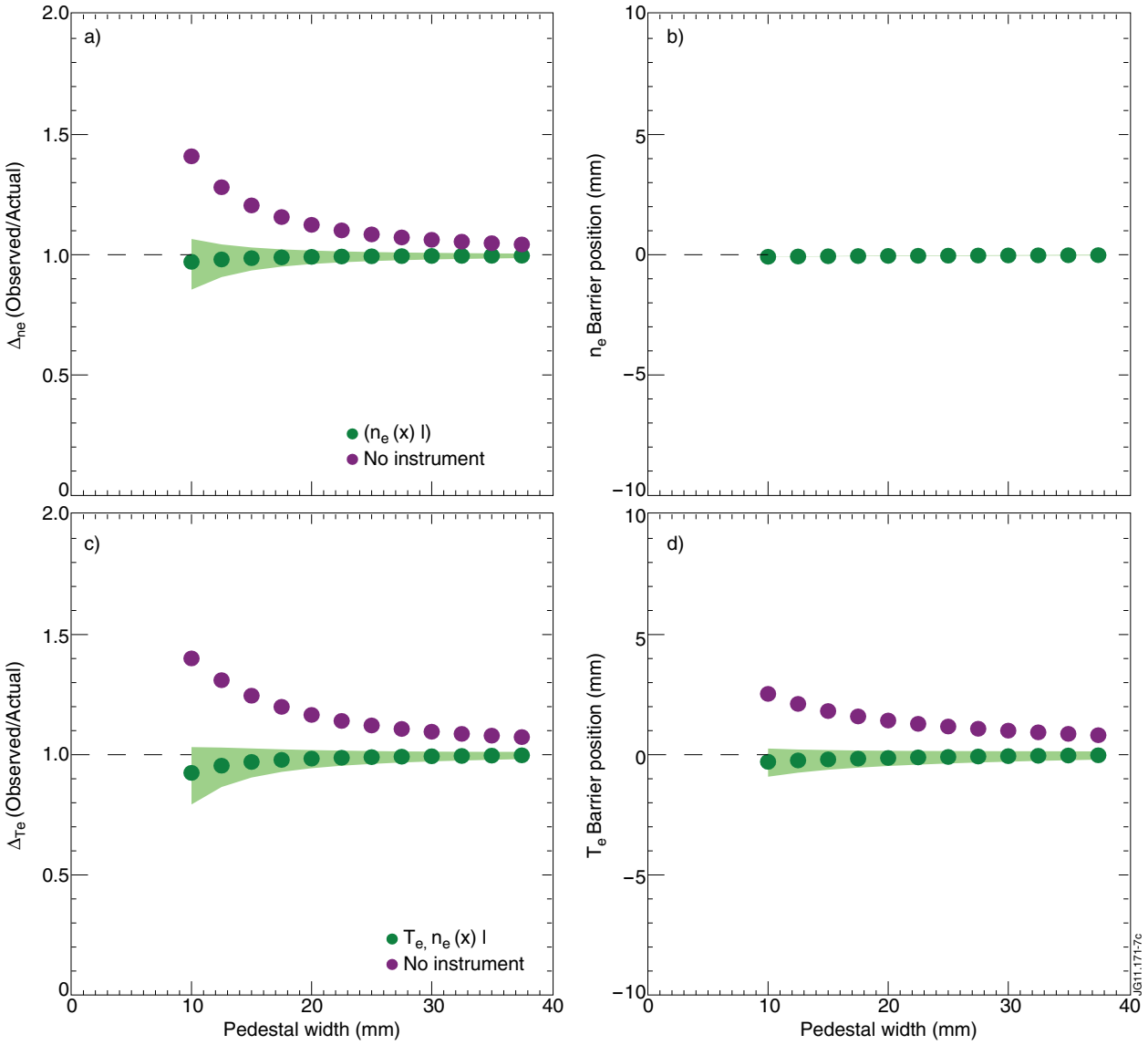

Figure 7: Simulation results using the present HRTS configuration (single fibre, f = 10m) for the pedestal fits without (purple) and with deconvolution (green dots) for (a) density pedestal width, (b) density pedestal position, (c) temperature pedestal width, (d) temperature pedestal position. Shaded areas represent the uncertainty.

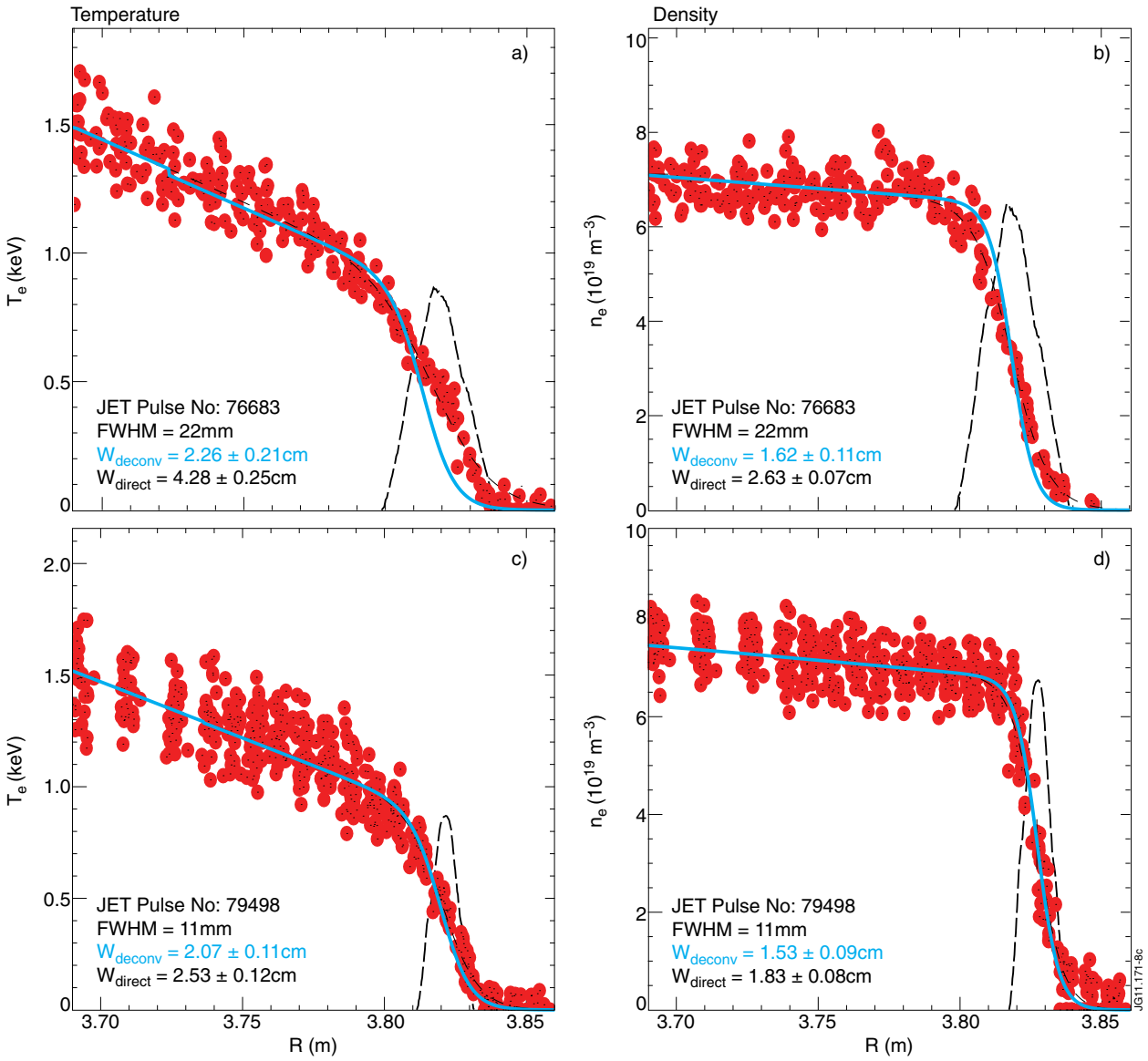

Figure 8: Pedestal fits for two similar JET plasmas, I_p = 2.5MA, B_t = 2.7T, δ = 0.42, P_{NBI} = 15MW and low gas fuelling. Frames (a) and (b) are respectively the profiles of temperature and density obtained with the original HRTS configuration. Frames (c) and (d) with the present configuration. The instrument functions are drawn in blue and green shaded areas for the original and present configurations respectively. The fits with deconvolution (blue line) and without deconvolution (dashed black line) are shown.

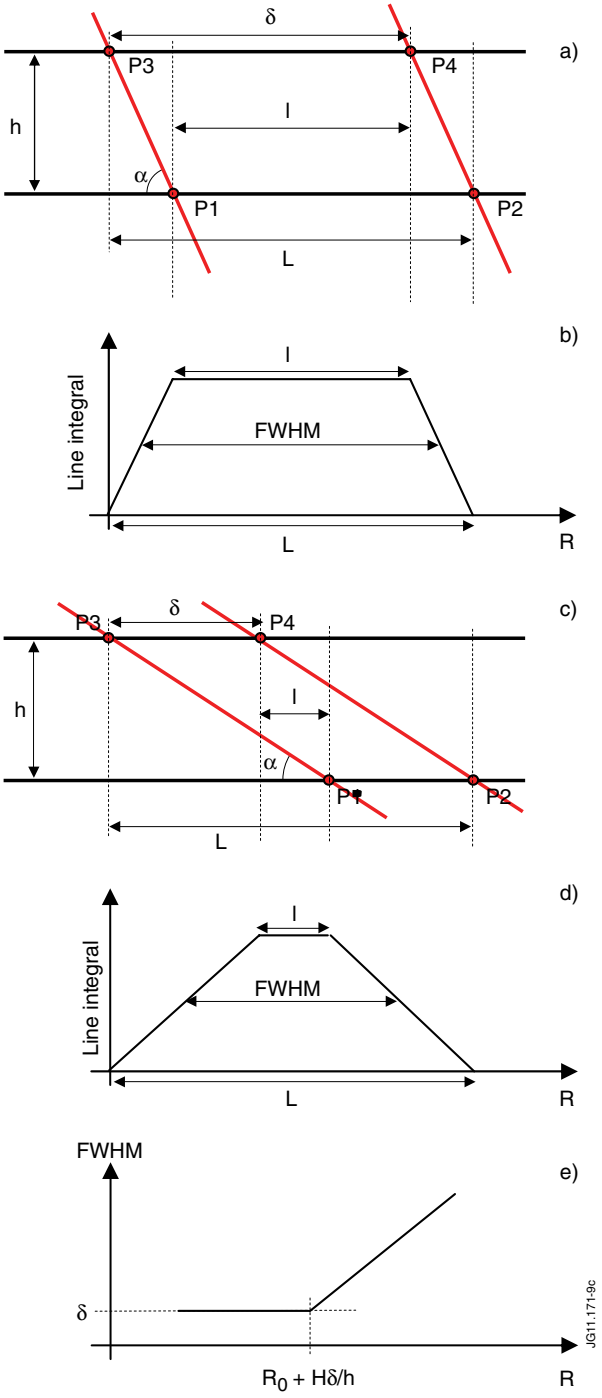

Figure 9: (a) Geometry relevant in the core region and (b) corresponding instrument function. (c) Geometry relevant in the pedestal and (d) corresponding instrument function. (e) Sketch of the FWHM versus the radial position of the scattering volume.